

The Unified Cluster Catalogue: towards a comprehensive and homogeneous database of stellar clusters

Gabriel I. Perren,^{1,3}★ María S. Pera,^{2,3} Hugo D. Navone^{2,3} and Rubén A. Vázquez^{1,4}

¹*Instituto de Astrofísica de La Plata, IALP (CONICET-UNLP), 1900 La Plata, Argentina*

²*Instituto de Física de Rosario, IFIR (CONICET-UNR), 2000 Rosario, Argentina*

³*Facultad de Ciencias Exactas, Ingeniería y Agrimensura (UNR), 2000 Rosario, Argentina*

⁴*Facultad de Ciencias Astronómicas y Geofísicas (UNLP), 1900 La Plata, Argentina*

Accepted XXX. Received YYY; in original form ZZZ

ABSTRACT

We introduce the Unified Cluster Catalogue, the largest catalogue of stellar clusters currently listing nearly 14000 objects. In this initial release it exclusively contains Milky Way open clusters, with plans to include other objects in future updates. Each cluster is processed using a novel probability membership algorithm, which incorporates the coordinates, parallax, proper motions, and their associated uncertainties for each star into the probability assignment process. We employ Gaia DR3 data up to a G magnitude of 20, resulting in the identification of over a million probable members. The catalogue is accompanied by a publicly accessible website designed to simplify the search and data exploration of stellar clusters. The website can be accessed at <https://ucc.ar>.

Key words: (Galaxy:) open clusters and associations: general – catalogues – methods: data analysis

1 INTRODUCTION

Open clusters (OCs) are groups of loosely gravitationally bound coeval stars with a wide range of masses, formed from the same molecular cloud. Their orbits generally position them close to the formal Galactic plane, although there are a few examples of OCs with large vertical distances. Having originated from the same cloud, their member stars share a common chemical composition and age, and are located within a somewhat compact region in space. The study of OCs holds fundamental importance for several key aspects in astrophysics research, including the process of stellar evolution as well as the dynamics, structure, formation, and chemical evolution of the Galactic disk (Friel 1995).

Catalogues of OCs are essential for organizing these objects into publicly available databases and, most importantly, as a tool for helping researchers discover new potential OCs while discarding false detections. Catalogued bonafide OCs are the most natural training dataset against which we can test and improve new algorithms for stellar clusters detection. There have been efforts to provide catalogues of OCs to the astrophysical research community at least since the late 18th century, even if that was not the primary objective of the compilation. The first of such well known catalogues to include OCs is the Messier Catalogue (Messier 1774) with less than 30 OCs listed. This work was quickly followed by Herschel’s Catalogue of One Thousand New Nebulae and Clusters of Stars (Herschel 1786), culminating a century later with Dreyer’s New General Catalogue of Nebulae and Clusters of Stars (NGC, Dreyer 1888). The NGC lists less than 650 OCs, which is more than twenty times the number of objects present in Messier’s catalogue.

After that first rapid growth the pace with which OCs were discovered and catalogued slowed down. The next big catalogue, again published almost a century later, was the Base Données Amas (Mermilliod 1995) which listed a little over 1100 OCs, based on the previous compilation by Lynga (1987). This work is the foundation of the WEBDA catalogue,¹ a heavily used resource in the analysis of OCs. In the following decade, with the advent of large public databases containing from hundreds of thousands to millions of stars (e.g., Hipparcos and Tycho (Perryman et al. 1997; Høg et al. 1997), as well as 2MASS (Skrutskie et al. 2006)), the task of detecting new candidate OCs became substantially more attainable. This is particularly true for those objects that are faint, obscured by dust, or not in the vicinity of the solar system. Catalogues such as the Milky Way Star Clusters (Kharchenko et al. 2012) or those presented by Loktin & Popova (2017) or Bica et al. (2019) increased the number of known OCs to more than 3000 in a few decades.

Currently, the release of the Gaia survey database (Gaia Collaboration et al. 2016) with over a billion observed stars has led to an enormous quantity of new candidate OCs being reported in the literature. Clustering algorithms such as HDBSCAN (Campello et al. 2013) are used for the automatic identification of overdensities, dramatically improving the detection sensitivity compared to manual methods. The latest catalogue that made use of both Gaia data and this algorithm is the one published in Hunt & Reffert (2023). It contains a little over 6000 OCs, ~2000 of which are new candidates. Just the current year, at the moment of writing this article, approximately 5000 new candidate OCs have been presented. In Fig. 1 we show the growth in catalogued OCs over the last two and a half centuries. The last two decades show an almost exponential trend, with no signs of

★ E-mail: gabrielperren@gmail.com

¹ <https://webda.physics.muni.cz/webda.html>

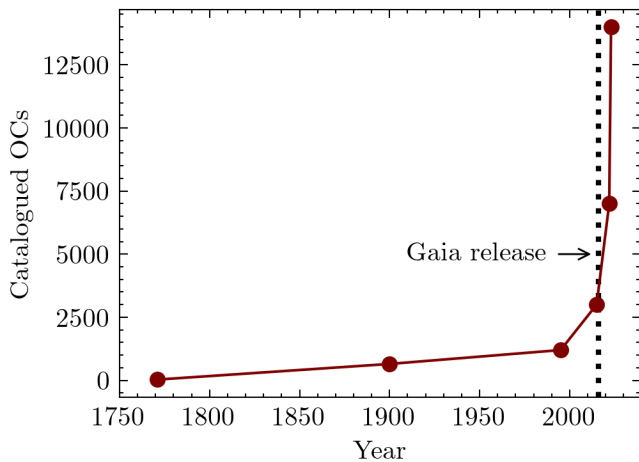


Figure 1. Approximate number of catalogued OCs in the literature from the late 1700s to the present day, including this work. The release date of Gaia’s survey data is indicated with a dotted line.

slowing down. Estimates for the total number of OCs in the Galaxy locate the upper limit over 10^5 (Bonatto et al. 2006), which means that there remain still a lot of objects waiting to be found.

Studies where thousands of new candidate OCs are introduced present a real challenge. Depending on the input parameters of the clustering algorithms employed in these works, apparent groupings of non-physically related stars can easily disguise themselves as OCs. Such false detections are prone to remain hidden in these catalogues since the number of objects is too large to allow a detailed individual analysis. Furthermore, authors are often unable to cross-reference their findings with other recent catalogues, due to the dispersion of information across articles and the influx of new articles published just months apart. This translates into duplication issues which, combined with the aforementioned problem, can have non trivial effects when these objects are used in massive studies (for example, when analysing the Galactic disk structure).

Our aim is to provide the community with a service that can be used to alleviate these issues. We combined, to the best of our knowledge, all the recent catalogues of OCs in the literature, and used them to generate a single catalogue of ~ 14000 unique OCs. We call this the Unified Cluster Catalogue (UCC hereafter). The UCC contains several thousands more objects than similar services such as WEBDA² and SIMBAD,³ which list ~ 1800 and ~ 5200 objects, respectively. Moreover, while neither WEBDA nor SIMBAD provide homogeneous membership information, we applied a new tool called fastMP⁴ to assign membership probabilities to each listed OC. The code was designed to work on the Gaia survey data, resulting so far in more than 1 million stars identified as probable members of the catalogued OCs. This gives us the largest homogeneously processed database of OC members to date. The data collected for each OC in the UCC catalogue, along with their estimated members, is publicly available in the website <https://ucc.ar>. This website will undergo periodic updates as new candidate OCs are introduced to the community.

This article is structured as follows. In Sect. 2 we introduce the

stellar cluster databases employed to generate this initial version of the UCC. Section 3 presents the new membership algorithm, fastMP, employed in the study of all the catalogued clusters. A comparison of our membership results with those recently published is performed in Sect. 4, along with the presentation of the public web site where these results will be hosted, updated, and expanded in the future. Finally, our conclusions are highlighted in Sect. 5.

2 DATABASES

We gathered the OCs listed in the literature up to the present day, extracted from 32 databases published in the last 11 years. The total number of entries is 24983, which were cross-matched to create a final catalogue of 13684 unique OCs. A few small databases were not added as they are included entirely in Hunt & Reffert (2023), these are: Zari et al. (2018), Bastian (2019), Tian (2020), Qin et al. (2021), Anders et al. (2022), Casado & Hundy (2023). Table 1 lists these 32 databases along with the number of OCs that were left in each, after extensive cleaning and sanitizing. To avoid cluttering the article we defer the details of these cleaning procedures to Appendix A, and restrict this section for a general discussion of the cross-matching process.

Unlike other works, such as the recent Hunt & Reffert (2023, HUNT23), we do not attempt to cross-match OCs present in different databases using their positions or astrometry. Instead, we standardize the names of the OCs in the 32 selected databases, and use these names to find matching entries across all of them. Although we do not attempt to find duplicate OCs via positions or astrometry cross-matching, we do use this data to identify and flag the most obvious duplicate entries. For example, the CWWDL 14677 candidate OC presented in Chi et al. (2023c) has coordinates and astrometry values estimated as: RA=0.9526°, DEC=-30.002°, pmRA=4.222 mas yr⁻¹, pmDE=18.721 mas yr⁻¹, plx=2.61 mas. This is marked in the UCC as a duplicate of the well known OC Blanco 1, which has almost identical coordinates and astrometry values in the literature: RA=0.9149°, DEC=-29.958°, pmRA=4.215 mas yr⁻¹, pmDE=18.724 mas yr⁻¹, and plx=2.59 mas. There are many entries with similar issues throughout the databases used to generate the UCC. Note that although cases such as this one are flagged as possible duplicates, they are not removed from our final catalogue. The rationale behind this decision is that the authors originally introduced these objects as new discoveries, and we choose to retain this nomenclature. Even when duplications are evident, we believe this decision can help future research in identifying structures that were incorrectly labelled as new OCs, thereby preventing the repetition of the same error. Labelling duplicates can also aid in the detection and analysis of binary cluster systems. We will show in Sect. 4 how each OC is assigned a probability of being a duplicate of others in the UCC catalogue, based on a simple set of rules. These rules, even if somewhat arbitrary, represent a reasonable initial step toward a more in-depth analysis of duplicate candidate OCs in the literature.

In Fig. 2 we show the distribution of the 13684 candidate OCs catalogued in the UCC to date, segregated by distance range. These distances are estimated as the inverse of the provided parallaxes. It is worth noting that many of the OCs in older catalogues, such as Kharchenko et al. (2012) and Bica et al. (2019), have no associated astrometry but can have distances estimated as part of the fundamental parameters analysis process (usually along with age and extinction). As illustrated in the upper-left plot, these catalogued OCs with no astrometry represent almost a quarter of the entire

² <https://webda.physics.muni.cz/>

³ <https://simbad.u-strasbg.fr/simbad/>

⁴ fastMP: <https://github.com/Gabriel-p/fastMP>

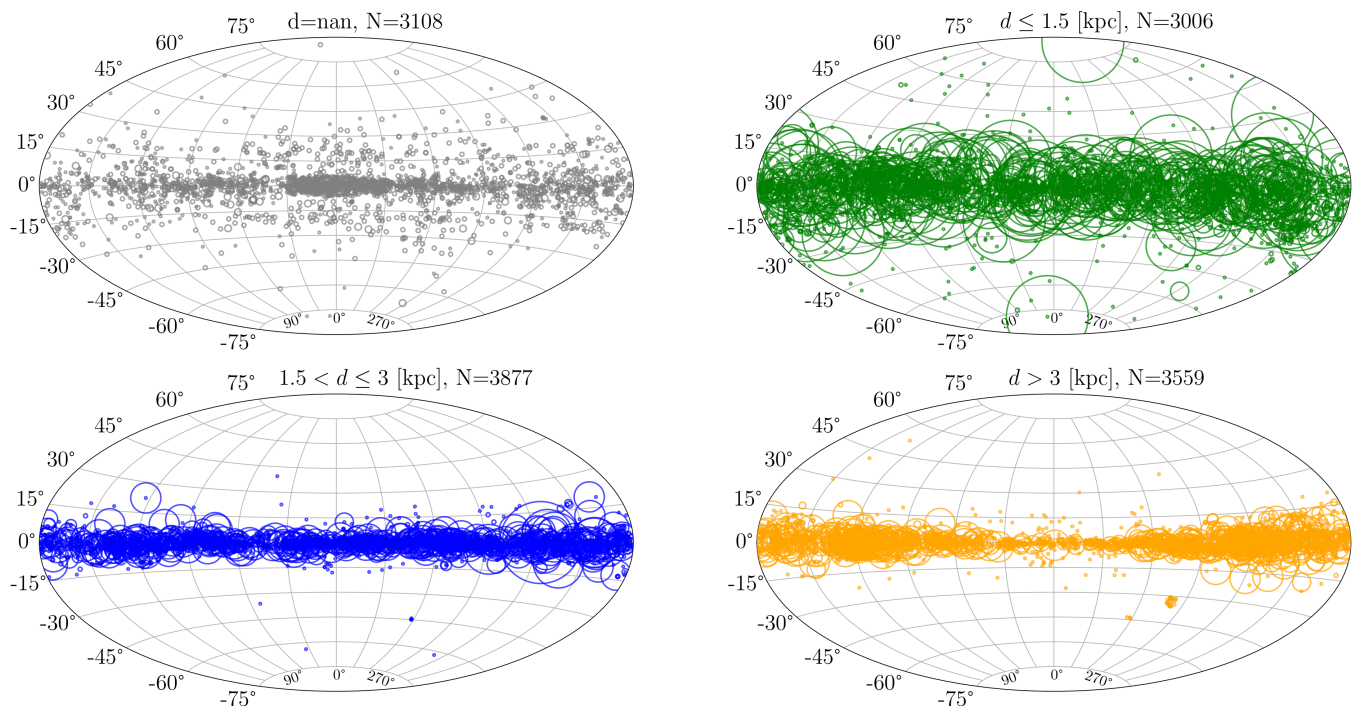


Figure 2. Map of the full database of catalogued OCs in this work. Positions displayed in galactic coordinates, segregated by range of catalogued distance. From top left to bottom right: OCs catalogued with no distance (grey), OCs with $d \leq 1.5$ kpc (green), OCs in the range $1.5 < d \leq 3$ kpc (blue), and OCs with $d > 3$ kpc (orange). The size of each candidate OC is proportional to the number of databases from Table 1 where it is included.

database. Expectedly, OCs catalogued at distances closer than ~ 1.5 kpc (as shown in the upper-right plot) are included in a significantly larger number of databases, indicated by the proportional sizes of the circles.

The UCC includes candidate OCs found through the analysis of infrared photometry, such as the FSR (Froeblich et al. 2007), Ryu (Ryu & Lee 2018), and VVV (Barbá et al. 2015) objects. These candidates are not included in any of the recent large scale catalogues like Cantat-Gaudin et al. (2020, CANTAT20) and HUNT23 because they are considered to be too faint to be detected by the usual clustering algorithms, using Gaia photometry. A large portion of the candidate OCs with no assigned distance seen in the upper-left panel of Fig. 2 are precisely these objects. Our method, as we will demonstrate in Sect. 3, does not rely on the capability of a clustering algorithm to detect faint and small overdensities, which it will most likely not be able to accomplish. Thus, we can include these candidate OCs in the UCC, and provide a first estimation of their mean positions in terms of proper motions and parallax.

In this initial version of the UCC we did not include information on candidate OCs identified as probable asterisms, presented, for instance, in Cantat-Gaudin & Anders (2020). The rationale behind this omission is the considerably dispersed nature of such information, rendering its collection more challenging compared to, for example, positional data or fundamental parameter values. We intend to incorporate this information in future updates to the catalogue. We do however assign two different quality classification parameters to each object, which can be used to identify likely non-clusters. This will be discussed in more detail in Sect 4.

Recently, Kounkel et al. (2020) presented a list of more than 8000 moving groups. Many of these are very extended and small groups which can hardly be classified as OCs. For this initial version of the

UCC, we decided to remove these groups from the catalogues where they are included, i.e. He et al. (2022b) and HUNT23.

While we were in the process of preparing this manuscript, a new work by He et al. (2023a) introduced ~ 2000 new candidate OCs, for which their associated data is not yet accessible. Although these candidate OCs are not included in the current version of the UCC, it is highly probable that they will have been incorporated by the time this article is published.

We utilized the most recent release of the Gaia survey data (DR3; Gaia Collaboration et al. 2022; Babusiaux et al. 2022) implementing a single filter with a maximum magnitude cutoff at $G=20$ mag. No additional filters were applied on this dataset, which was employed for the processing of the entire catalogue, extracting the most probable members for each listed OC. In Sect. 3 we elaborate on this process of membership probability estimation.

3 MEMBERSHIP METHOD

Once the databases listed in Table 1 are cross-matched and the final catalogue with unique entries is generated, our next objective is to compile a homogeneous database of likely member stars for each unique candidate OC. Typically, tools known as clustering algorithms are employed for this task. Three of the most frequently used clustering algorithms in the stellar cluster literature are Friends-of-Friends (Huchra & Geller 1982, FoF), DBSCAN (Ester et al. 1996) and HDBSCAN. Examples of recent articles listed in Table 1 where these algorithms are employed are Liu & Pang (2019), He et al. (2023b), and HUNT23, for FoF, DBSCAN, and HDBSCAN, respectively. More specialized tools such as UPMASK (Krone-Martins & Moitinho 2014) or our own recently developed pyUPMASK (Pera

Table 1. List of all the catalogues cross-matched in this article to generate the UCC database. Columns ID and N are the denomination used for new candidate OCs, and the total number of OCs taken from each work, respectively.

Reference	ID	N
Kharchenko et al. (2012)	–	2854
Loktin & Popova (2017)	LP	1050
Castro-Ginard et al. (2018)	UBC	23
Bica et al. (2019)	Bica	3555
Castro-Ginard et al. (2019)	UBC	53
Sim et al. (2019)	UPK	207
Liu & Pang (2019)	FoF	76
Ferreira et al. (2019)	UFMG	3
Castro-Ginard et al. (2020)	UBC	570
Ferreira et al. (2020)	UFMG	25
Cantat-Gaudin et al. (2020)	–	2017
Hao et al. (2020)	HXWHB	16
Ferreira et al. (2021)	UFMG	34
He et al. (2021)	HXHWL	74
Dias et al. (2021)	–	1742
Hunt & Reffert (2021)	PHOC	41
Casado (2021)	Casado	20
Jaehnig et al. (2021)	XDOCC	11
Santos-Silva et al. (2021)	CMA	5
Tarricq et al. (2022)	–	467
Castro-Ginard et al. (2022)	UBC	628
He et al. (2022a)	CWNU	541
He et al. (2022b)	CWNU	836
Hao et al. (2022)	OC	703
Li et al. (2022)	LISC	61
He et al. (2023b)	CWNU	1656
Hunt & Reffert (2023)	HSC	6272
Qin et al. (2023)	OCSN	101
Li & Mao (2023)	LISC	35
Chi et al. (2023b)	CWWL	46
Chi et al. (2023a)	LISC-III	82
Chi et al. (2023c)	CWWDL	1179
Number of OCs in all the catalogues		24983
Number of unique OCs after cross-matching		13684

et al. 2021, a generalized Python-based version of UPMASK), also depend at their cores on these clustering algorithms.⁵ While these tools have been used extensively in the literature, we believe they have some important shortcomings that need to be addressed. The first one is the processing time. For the amount of data we are handling, efficient code is crucial. For example, it took HUNT23 eight days of runtime on 48 CPU cores to process the Gaia DR3 database using HDBSCAN. This large requirements can easily become an obstacle in the analysis. Second, and tightly related to the first problem mentioned previously, these algorithms do not take uncertainties into account. One could incorporate uncertainties associated with the input data through a bootstrapping mechanism (Efron 1979), but the initial problem would still persist. If a single data processing run is very time-consuming, as shown above with the HDBSCAN example in HUNT23, conducting thousands of runs becomes virtually impossible. Finally, the definition of what constitutes a cluster is often overlooked in most (if not all) works related to stellar membership

⁵ UPMASK depends on the K-Means (MacQueen 1967; Lloyd 1982) algorithm, while pyUPMASK is able to work with about a dozen different clustering algorithms.

estimation. This is mainly due to the absence of a standardized definition across different clustering algorithms, with each algorithm employing its own definition. When applying these algorithms, selecting cluster members depends on several unique parameters specific to the method used. Setting values for these parameters is not straightforward, and their choices often lack a strong justification other than producing “reasonable” results.

The ideal scenario would provide a database containing both mass and coordinates for each star in full phase space, encompassing three positional and three momentum variables. This would allow us to define a cluster that properly accounts for the gravitational potential of the Galaxy. However, this ideal situation is not the case. We lack information on masses, and even the phase space is incomplete due to the absence of radial velocities in the vast majority of cases,⁶ What we have for each observed stars is thus a 5-dimensional data point made up of coordinates (equatorial, galactic), parallax, and proper motions. With this at our disposal, we propose the following general definition of cluster:

Given an integer value $m > 0$ and a point c in an n -dimensional space, a “cluster” is defined as the collection of m elements with the smallest n -dimensional Euclidean distance to c .

The advantage of explicitly stating a definition of a cluster is that we no longer depend on different clustering methods or their extraneous parameters. Assuming the centre and the estimated number of members are given, this definition will always yield the same set of selected stars as probable members. This is true at least approximately, since uncertainties do play a role here as we will see below.

Taking into account the aforementioned shortcomings of general clustering algorithms, we decided to develop a new tool for estimating membership probabilities which we have named `fastMP` (acronym for *fast Membership Probabilities*), based on the previously outlined definition of a cluster. We named the code `fastMP` due to its processing speed. In our extensive testing, it took `fastMP` less than 3 seconds on average to analyse an OC in an 11 years old 4-cores CPU. This means that the entire UCC (almost 14000 OCs so far) can be processed in approximately 11 hours on a very modest CPU. It should be noted that this estimate includes the time required for incorporating uncertainties into the process. In Fig. 3 we present the configuration of the fundamental blocks within the `fastMP` algorithm. As can be seen, it is a rather straightforward process primarily reliant on the two basic parameters mentioned in the cluster definition: its central coordinates and the number of members.

We briefly describe each individual block in the following subsections. The code is entirely open source and distributed under the GNU General Public License version 3 (GPL v3),⁷ meaning that it can be easily tested and modified.

3.1 Centre estimation

To estimate the most likely centre c for the OC under analysis, `fastMP` uses a three step process. First, it searches for the region of maximum density in proper motions. Only the 2-dimensional space of proper motions is employed here since this is generally where the overdensity

⁶ Currently Gaia contains radial velocity data for less than 2% of the observed stars, see: <https://www.cosmos.esa.int/web/gaia/dr3>.

⁷ <https://www.gnu.org/copyleft/gpl.html>

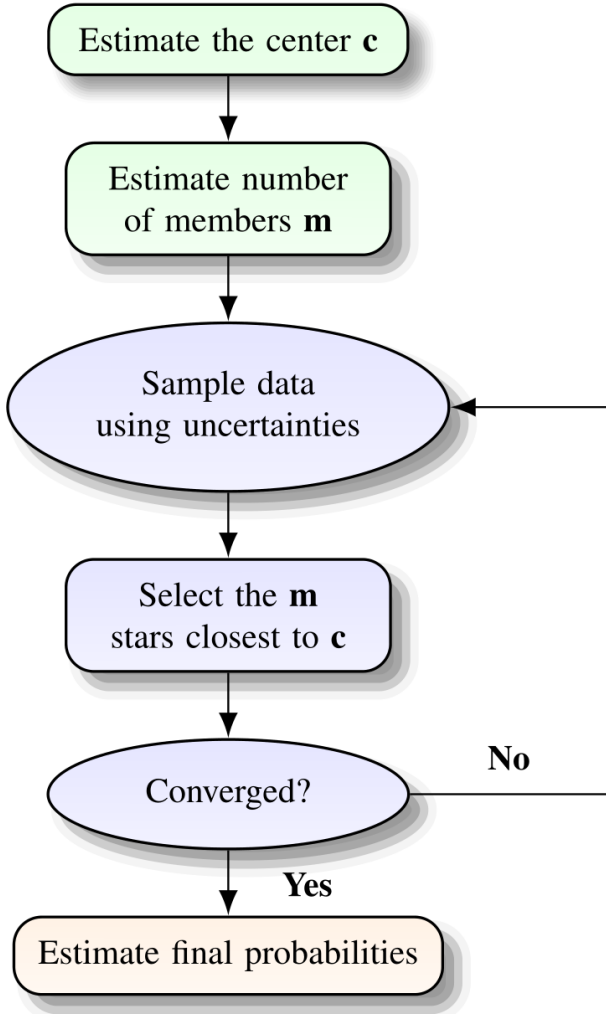


Figure 3. Basic flow chart of the algorithm used by our *fastMP* membership estimation tool.

is most visible, standing out against the surrounding stars in the observed field. The position of the overdensity is found through an iterative process that starts with the full set of data, and gradually “zooms in” until a convergence criterion is reached. The second step selects a subset of stars with the closest distance to these centre coordinates in proper motions space. In the third step, the final centre value is obtained using a *k*-nearest neighbours algorithm to select the point with the largest density in the 5-dimensional space (coordinates, parallax, proper motions).

3.2 Number of members estimation

Once the centre point is estimated, the total number m of stars that can be considered members of the OC is obtained through Ripley’s *K* function (Ripley 1976, 1979). This function is used to assess how close a group of points is to a random uniform distribution. We refer the reader to our previous article where we presented *pyUP-MASK* (Pera et al. 2021), where we introduced the concept in much more detail. Subsets of stars are selected in rings, moving outward from the centre values estimated in proper motions and parallax. If these stars are considered to be far enough from a random uniform

distribution in coordinate space, they are kept as probable members of the OC. In this block we can also reject stars that are more likely to belong to other clusters in the frame, to more accurately estimate the true number of members for the OC under analysis.

Since it is run only once, Ripley’s *K* function can be replaced by any other method to estimate the size of a cluster (for example some of the already mentioned clustering algorithms) without much impact on the performance. It can even be skipped entirely by feeding this number to *fastMP*, estimated manually or by some external process, as explained in the final paragraph of this section.

3.3 Sampling, selection, convergence

This is the bootstrap block where we incorporate the data uncertainties into the final membership probabilities. Its basic function is to sample the observed data using its uncertainties, select those m stars closest to the centre c , and finally repeat this process until a convergence criterion is reached. We define as a stopping condition the run when the total number of stars with probability greater than 50% has stabilized for several runs. The bootstrap block is usually run a few hundred times before convergence is achieved.

3.4 Membership probabilities

To estimate the membership probability for each star, the algorithm simply divides the number of times a given star was selected in the bootstrap block by the number of runs required until convergence. In cases where no star was selected by the bootstrap block, probabilities are assigned based on the 5-dimensional distances to the centre. These are lower quality probabilities since they do not make use of the uncertainties of the data. This last-resort option is only employed for candidate OCs that are too faint to be observed, meaning that their members do not form a region dense enough to distinguish them from the background of field stars.

Finally, it is worth noting that an important advantage of *fastMP* over tools commonly used like *UPMASK*, *pyUPMASK*, *HDBSCAN*, etc., is that it can run in supervised mode. In this context, we make the distinction between supervised and unsupervised in the sense that the algorithms mentioned above work with no prior information about the cluster(s) being analysed. We call this “unsupervised”. In contrast, *fastMP* allows information about the cluster to be passed along with the input data. We call this “supervised”. Such information can be the centre of the cluster, its total number of members, or both. If any of these values are fed to the code after estimating them manually or via an external method, then its corresponding block (either centre or number of members estimation) is skipped. This is of great help, particularly for OCs that are very faint or sparse and cannot easily be picked up by the usual clustering algorithms. It is also a feature that allows the code to analyse systems that are very close together, either in positional space or a combination of this and the proper motions and/or parallax dimensions, by fixing its centre and/or the number of constituent members. In the following section we show that *fastMP* has an excellent performance when compared to recent works that generate lists of members for OCs, like *CANTAT20* and *HUNT23*.

4 RESULTS

This section is divided as follows. In Sect. 4.1 we analyse the issue of duplicated entries across catalogues. Sect. 4.2 compares the results of our membership estimation with those from recent large catalogues.

Sect. 4.3 discusses a possible classification of the candidate OCs as real physical objects to separate them from artefacts derived from the application of different clustering algorithms. Finally, Sect. 4.4 presents a brief overview of the online service where this catalogue is hosted and a few of the issues that will be improved in the future.

4.1 Duplicates

One of the main problems with today’s state of research in the area of OCs is, as mentioned earlier, the large number of articles being published on the subject. This should not be a concern a priori, but with articles appearing every few months presenting new candidates by the thousands, keeping track of the latest proposed objects becomes a not so simple task. This is evidenced by the large number of potential duplications that can be found when cross-matching the most recent databases with older ones.

In this work we do not attempt to merge and/or discard candidates as duplicates, as this is not a trivial assessment to make. The UCC only flags OCs that have the potential of being duplicates of others, following a parallax-based decision rule. This rule checks the distance from a given OC to all the others in the catalogue in three separate components: coordinates (arcmin), parallax (mas), and proper motions (mas yr⁻¹). If these distances are smaller than a given threshold, they are converted into a probability using a linear relation. If they are larger than the threshold, they are assigned a probability of zero.⁸ The relations depend on the distance to the OC (estimated from its catalogued parallax) and can be seen in the block below.

```

if parallax >= 4
    xy_r, plx_r, pm_r = 20, 0.5, 1
else 3 <= parallax < 4
    xy_r, plx_r, pm_r = 15, 0.25, 0.75
else 2 <= parallax < 3
    xy_r, plx_r, pm_r = 10, 0.2, 0.5
else 1.5 <= parallax < 2
    xy_r, plx_r, pm_r = 7.5, 0.15, 0.35
else 1 <= parallax < 1.5
    xy_r, plx_r, pm_r = 5, 0.1, 0.25
else .5 <= parallax < 1
    xy_r, plx_r, pm_r = 2.5, 0.075, 0.2
else parallax < .5
    xy_r, plx_r, pm_r = 2, 0.05, 0.15
else parallax < .25
    xy_r, plx_r, pm_r = 1.5, 0.025, 0.1
else parallax is nan
    xy_r, pm_r = 2.5, 0.2

```

Here, xy_r , plx_r and pm_r are the parallax-based thresholds for each component (in arcmin, mas, and mas yr⁻¹, respectively). For example, if a candidate OC named A has a catalogued parallax of 0.75 mas, then xy_r , plx_r , $pm_r = 2.5, 0.075, 0.2$. This means that if there exists an OC named B with distances to A smaller than those thresholds, A and B will have a non zero probability of being duplicates of the each other. These rules for finding possible duplicates translate smaller distances to larger

⁸ If the distances in all three components between the OC and another object are zero, then the probability of these two being duplicates of each other is 1. If all three distances are beyond the maximum limits shown in the parallax-based rules, then the probability of duplication is zero. Distance values beyond zero and these limits are converted linearly in the probability range (0, 1).

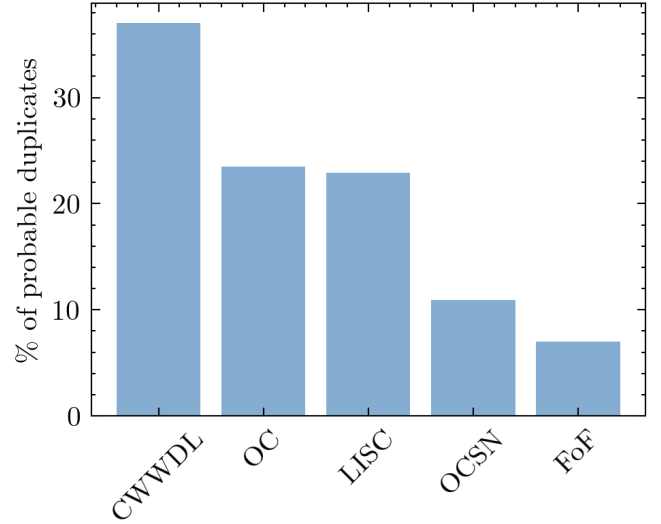


Figure 4. Percentage of probable duplicates for five recent databases of candidate OCs presented in the literature, characterized by their IDs. See Table 1 to match the corresponding article(s) to each ID.

probabilities. The reason for splitting the threshold into parallax ranges is that the farther away the OC the smaller its parallax, coordinates radius, and mean proper motions will tend to be. These thresholds and parallax ranges are of course entirely arbitrary, but we have observed very reasonable results using them. Employing this rule, if the catalogued positions are used, the aforementioned OC candidate CWDDL 14677 is flagged with a 65% probability of being a duplicate of Blanco 1. If we use the values for the main coordinates, proper motions, and parallax obtained from the most likely members found by fastMP instead, this probability increases to 84%.

In Fig. 4 we show the percentage of entries flagged as probable duplicates for five of the latest articles mentioned in Table 1. We selected as probable duplicates those entries with an assigned probability larger than 50%. The CWWDL clusters from Chi et al. (2023c) stand out with almost 40% of its 1179 candidate OCs flagged as probable duplicates of entries in previous (older) catalogues. This is a rather large value that translates to more than 400 of the candidate OCs listed in this catalogue.

An example of two candidate OCs flagged as possible duplicates, with a probability value of 50% and 90%, are CWWDL 578 Chi et al. (2023c) and LISC 3279 (Li et al. 2022). These objects were associated by our parallax-based rule to two UBC OCs, presented in Castro-Ginard et al. (2020). The five dimensional positions catalogued values for these four entries are shown in Table 2. While we acknowledge that a simple rule based on distances in the coordinates, parallax, and proper motion spaces is not a substitute for a thorough and detailed analysis of duplications, it can certainly serve as a reasonable starting point. Studies involving binary clusters systems can also rely on these probabilities for their initial assessment. In total, there are over 2000 entries in the UUC flagged as either duplicates or flagged for having one or more duplicates. This accounts for ~15% of the entire catalogue.

Table 2. Examples of two pairs of OCs flagged as duplicates by our parallax-based rule with probabilities of 50% (1st and 2nd columns) and 90% (3rd and 4th columns).

	P \approx 50%		P \approx 90%	
	CWDDL 578	UBC 395	LISC 3279	UBC 361
RA	345.743	345.655	290.000	290.016
DEC	57.231	57.206	15.146	15.157
Plx	0.412	0.409	0.630	0.632
pmRA	-2.844	-2.869	-1.669	-1.701
pmDE	-2.542	-2.591	-5.225	-5.232

4.2 Membership analysis

More than one million estimated members are stored in this initial version of the UCC. This is almost half a million more than those found in the HUNT23 catalogue (after removing globular cluster and moving groups), and approximately five times the number in CANTAT20. The latter database is expected to contain fewer entries not only because it lists a smaller number of OCs, but also because it only reaches a magnitude of $G=18$ mag, whereas UCC and HUNT23 go two magnitudes deeper.

In the top plot of Fig. 5, we show the distribution of estimated members for these three catalogues as a function of Gaia’s G magnitude. The central plot shows the same distributions but normalized by the total number of entries in each catalogue. Finally, the bottom plot displays the percentage of members in CANTAT20 and HUNT23 that match members estimated by the UCC. In this plot CANTAT20 shows an overall match in the range 75-80% across the entire magnitude range, up to its maximum of $G=18$ mag. The match with HUNT23 remains around 70-75% up to $G\approx 17$ mag, after which it starts to decline. For the largest magnitude in UCC and HUNT23, $G=20$ mag, the match percentage is $\sim 35\%$. This can be primarily explained by two processes. On one hand, the large sensitivity of the HDBSCAN algorithm often causes it to return false positives, as reported by HUNT23. This can result in an overestimation of the number of members assigned to each candidate OC. On the other hand, the methods employed in CANTAT20 and HUNT23, namely UPMASK and HDBSCAN, respectively, do not take into account the uncertainties in Gaia’s data, while *fastMP* does. Incorporating uncertainties into the membership probability estimation has the most significant impact on stars in the lower mass region, as they have the largest errors. The *fastMP* code also adopts a more cautious approach when estimating the total number of stars associated with a given OC, based on Ripley’s K function, as mentioned in Sect. 3.2. The central plot in Fig. 5 clearly illustrates these effects, where normalizing by the number of OCs in each catalogue causes the UCC’s distribution dip below those of CANTAT20 and HUNT23. The UCC averages ~ 90 members per OC, HUNT23 has around ~ 110 members per OC, and CANTAT20 is close to ~ 95 members per OC.

4.3 Classification

Determining what constitutes a genuine physical cluster of stars is not an easy task when dealing with OCs (Parker 2014). Whereas globular clusters comprise hundreds of thousands of member stars, OCs are significantly smaller. In the previous section we demonstrated that a reasonable average for the number of members within an OC is ~ 100 stars, with a pronounced bias toward smaller values. A comprehensive physical analysis to ascertain whether a few dozen stars are gravitationally bound requires information that we

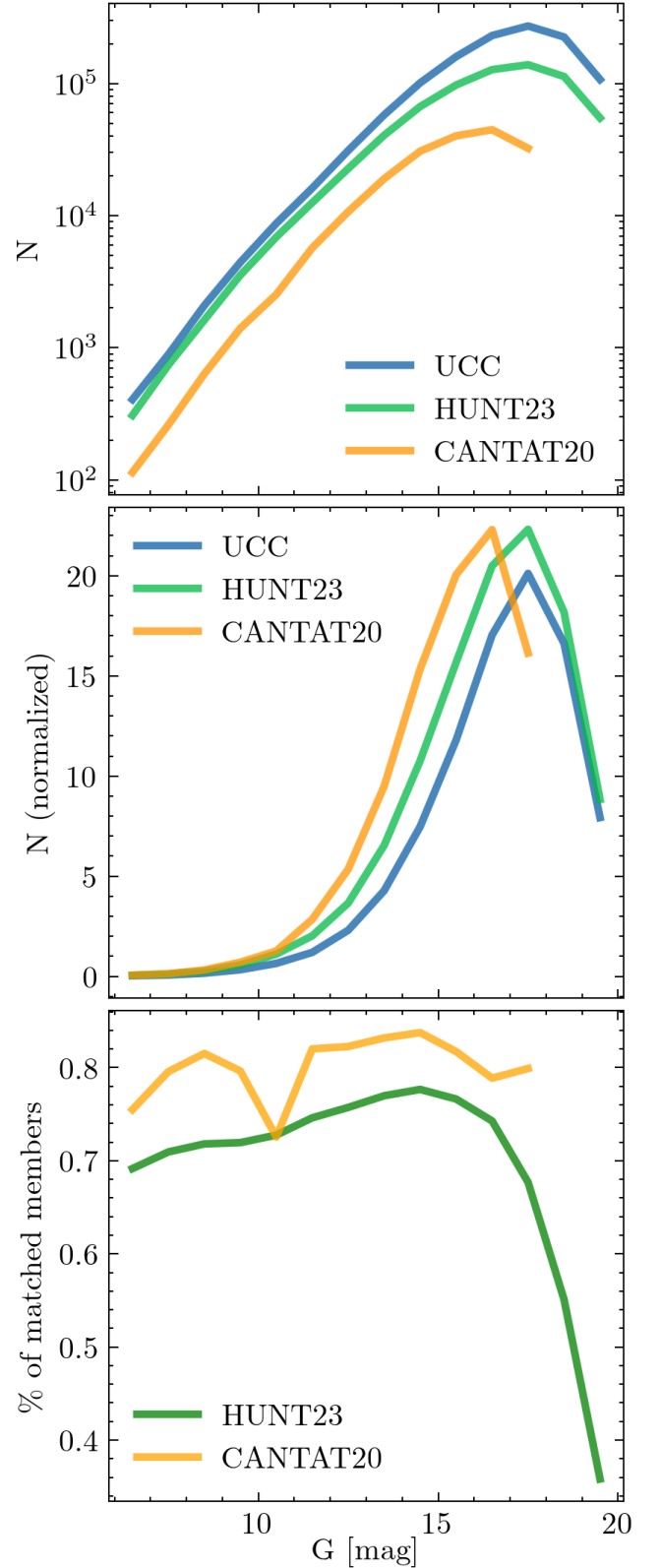


Figure 5. Top: total number of identified members versus magnitude, for the catalogues HUNT23, CANTAT20, and the UCC. Centre: same as above but normalized by the total number of entries in each catalogue. Bottom: percentage of members in HUNT23 and CANTAT20 matched with members identified by the UCC, versus magnitude.

currently lack. For example, the definition presented in [Gieles & Portegies Zwart \(2011\)](#) requires a reliable estimation of total mass, age, effective radius, and eventually precise velocities.

This fact notwithstanding, there are still methods we can employ to approximate a comprehensive dynamical analysis for characterizing candidate OCs as more or less likely to be genuine. Two of these methods, or quality criteria, were proposed by [Cantat-Gaudin & Anders \(2020\)](#). The first method is based on setting an upper limit for the internal velocity dispersion of OCs. Beyond this limit, objects are expected to either be globular clusters or unbound groups. Initially, this limit is set conservatively at 5 km s^{-1} . However it is relaxed to 1 mas yr^{-1} for candidate OCs located beyond $\sim 1000 \text{ pc}$, where uncertainties in proper motions tend to dominate the measured values. We set the transition between both these limits at $\sim 1.5 \text{ kpc}$, which is the distance at which the velocity dispersion lines mentioned earlier intersect. The second method involves measuring the internal spatial dispersion of an OC. According to [Cantat-Gaudin & Anders \(2020\)](#), for the majority of confirmed OCs, the maximum dimension containing half the members is estimated to be $\sim 15 \text{ pc}$. The authors of HUNT23 slightly relax this condition to 20 pc , which we also adopt here. In [Fig. 6](#) we display the results of both of these approaches for approximating a “true OC region” using the data collected in the UCC, as well as the data presented in CANTAT20 and HUNT23. As can be seen, the region occupied by all three catalogues is very similar, with the UCC showing a broader distribution in total proper motion dispersion beyond $\sim 1000 \text{ pc}$. Nevertheless, the majority of candidate OCs fall well below the proposed quality criteria lines in both plots. Objects with large proper motion dispersions are mostly candidates listed only in the [Kharchenko et al. \(2012\)](#) catalogue which, to the best of our knowledge, have never undergone a proper analysis. There are also ~ 30 infrared candidates OCs from [Ryu & Lee \(2018\)](#) for which membership estimation is poor.

An example of an object located beyond the quality line for proper motion dispersion is NGC 7826, as identified in the top plot of [Fig. 6](#). While this object was found to not be a genuine OC in [Kos et al. \(2018\)](#) and classified as an asterism in [Cantat-Gaudin & Anders \(2020\)](#), we include it in the UCC as it is listed as an OC in the [Loktin & Popova \(2017\)](#) catalogue. As expected, the proper motion distribution of its most likely associated stars also places it outside the defined “true OC region” in this study.

We can also define other metrics to classify candidate OCs as more or less likely to be true physical objects, based on their estimated members’ data. The first metric we developed is a density-based classification, denoted as C_{dens} , and the second one is a photometry-based classification, denoted as C_{phot} . These metrics bear conceptual similarities to the CST score and CMD class defined in HUNT23, respectively. The density-based metric compares the distribution of member stars to that of nearby field stars in the 5-dimensional space of coordinates, proper motions, and parallax. The reasonable expectation is that neighbouring cluster members should exhibit smaller average distances than neighbouring field stars. Photometric data is processed separately because member stars of an OC in a colour-magnitude diagram (CMD) do not cluster around a central value, as they do in other data dimensions. Instead, they are distributed along an elongated path across the evolutionary sequence. For this reason we do not employ a closest-neighbour density-based method, but one based on the likelihood of the members’ sequence being equivalent to a random sequence drawn from field stars. To quantify this we utilize the same function developed for our ASTeCA package ([Perren et al. 2015](#)), which is based on the Poissonian distribution likelihood defined in [Tremmel et al. \(2013\)](#). In [Fig. 7](#), the

distribution of these two metrics is shown. They are both normalized within the $[0, 1]$ range, where 1 indicates a higher likelihood of being a collection of related cluster member stars for either metric. The colour is assigned based on the vertical distance to the quality line in the total proper motion dispersion diagram shown in the top plot of [Fig. 6](#). Objects that fall beyond this limit (i.e., displaying larger proper motion dispersion than that allowed for an OC) have values below zero and are drawn in purple. The sizes of the markers correspond to the spatial extension of the estimated members. A clear trend is evident where candidate OCs with larger C_{dens} values tend to have large C_{phot} values, as expected. There is also a visible dispersion around the 1:1 identity relation, indicating these two metrics are not entirely correlated. This lack of correlation is desirable, as it ensures that both methods provide distinct information. Objects with large total proper motion dispersions are mostly associated with low C_{dens} values but tend to span the entire range of C_{phot} values.

We combine these two classification metrics into a single quality class for each candidate OC to provide a quick overview of the characteristics of the catalogued objects. First, we divide the $[0, 1]$ range for both metrics into four equal-length segments (from 0 to 0.25, from 0.25 to 0.5, etc.) and assign a letter to each segment. The assignments range from D for the $[0, 0.25]$ segment to A for the $[0.75, 1]$ segment. These two letters, one for each metric, are then combined to generate a single class out of 16 possible combinations. The letter corresponding to the C_{phot} value is placed first, followed by the letter obtained for the C_{dens} value for each object. The better quality clusters are thus assigned AA classes while lower quality ones receive DD classes. The complete distribution of these classes is shown in [Fig. 8](#). The three highest quality classes (AA, AB, and BA) encompass over 5300 objects, constituting $\sim 40\%$ of the catalogue. In contrast the three lowest classes (CD, DC, and DD) contain nearly 2000 candidate OCs, equivalent to $\sim 15\%$ of the UCC. Classes AD and DA are among the least populated, suggesting that it is unlikely to encounter an object with a large value in C_{phot} and a low value in C_{dens} or vice versa, as one would expect.

In [Fig. 9](#) we present examples of four OCs listed in the UCC, each assigned combined classes of AA, BB, CC, and DD. The distinction between the better AA and the lower-quality DD classes is evident, both in the denser spatial, proper motions, and parallax distributions, as well as in the more defined cluster sequence observed in the CMD. It is important to note however that these quality cuts and classification methods, while valuable, are not sufficient to entirely replace a proper analysis of a candidate OC. They serve as guides to identify problematic cases, but their effectiveness still relies heavily on the precision of the membership estimation process. In cases where this process performs poorly, especially for more complex cases, the results may be compromised. Improved data quality for observed stars in the near future will hopefully enhance the effectiveness of these methods.

4.4 Overview of the service

To facilitate cross-catalogues identification of entries, each candidate OC in the UCC is assigned a unique name following the specifications of the International Astronomical Union. The naming convention is formatted as *UCCGLLL.LsBB.B*, where *UCC* represents the catalogue’s name, *G* indicates the use of galactic coordinates, *LLL.L* is the (truncated) longitude for the object, *s* is the sign of its latitude, and *BB.B* is the (truncated) latitude. In cases where two objects share the same coordinates, a lowercase letter from a to z is appended to the end of the name.

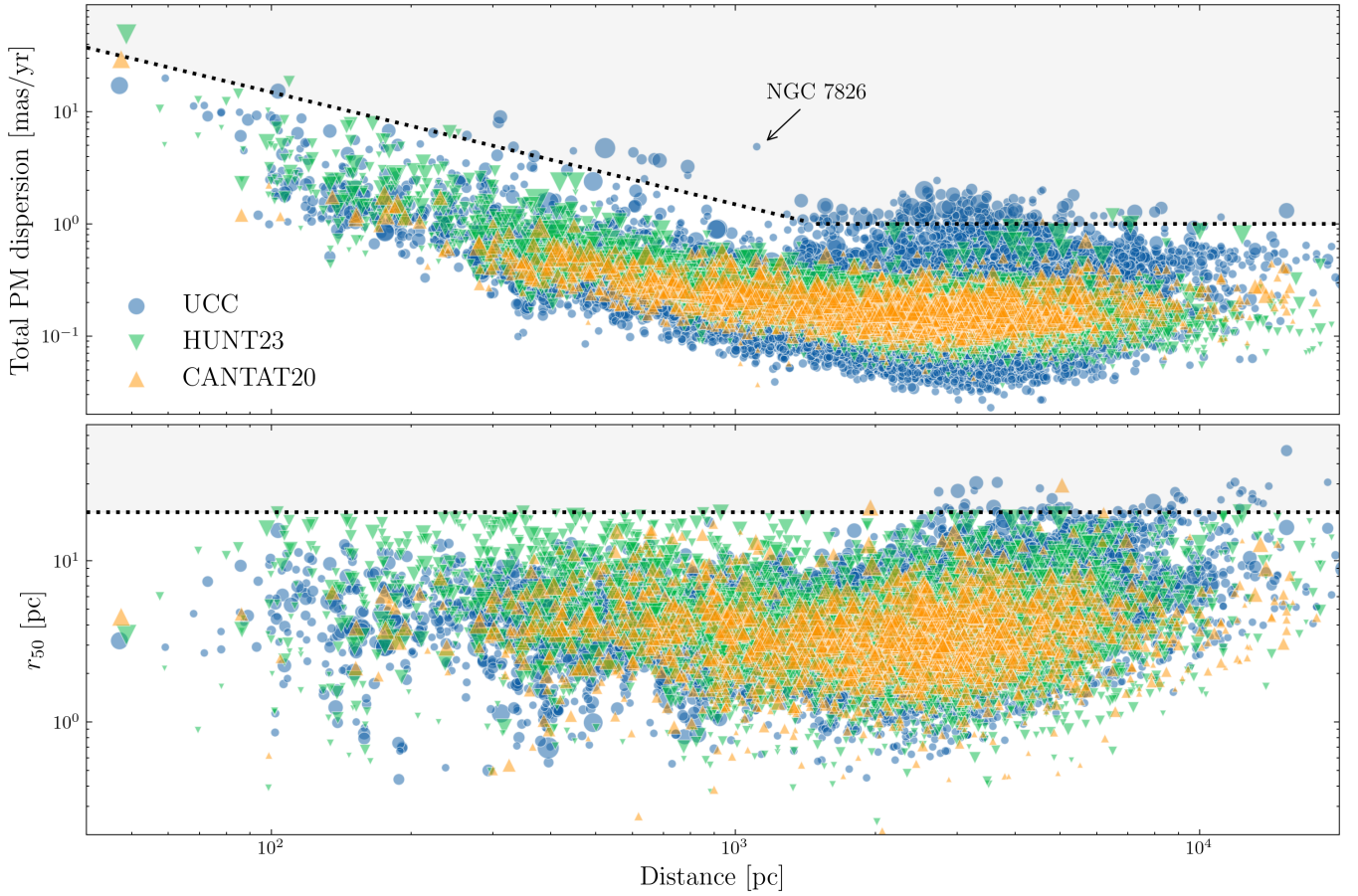


Figure 6. Distribution of total proper motion dispersion (top) and radius that contains half the members (bottom) versus distance, for the candidate OCs listed in CANTAT20 (orange), HUNT23 (green), and the UCC (blue). Sizes are proportional to each candidate’s associated number of members. The grey region in both plots is the “not true OC region” defined by the rules proposed by Cantat-Gaudin & Anders (2020).

The spatial position of each entry in the catalogue is displayed using Aladin’s visualization tool,⁹ showcasing coordinates, proper motions, parallax, and radial velocity values when available in the literature. Links to search the cluster’s main name in the SAO/NASA Astrophysics Data System (ADS),¹⁰ as well as links to perform a region search in the Strasbourg astronomical Data Center (CDS)¹¹ are provided. A Python notebook hosted on Google’s Colaboratory service¹² is made available, enabling users to interactively explore the Gaia survey data of each candidate’s estimated members. In this initial version the UCC only contains membership data obtained through our `fastMP` tool. However, in future updates we plan to include members estimated by other works, such as those from CANTAT20 and HUNT23, as well as the most recent catalogues.

Fundamental parameters like distance, extinction, age, and metallicity are also presented when available, sourced from various databases. These details will be expanded upon in future UCC updates as more values from the literature are incorporated. For each candidate OC nearby entries and potential duplicates are displayed,

along with the probability of being a duplicate, as explained in Sect. 4.1.

In an upcoming version of the UCC we will include individual notes on OCs, whenever available. Obtaining these notes is challenging as they are scattered throughout the literature rather than compiled in databases. For example Cantat-Gaudin & Anders (2020) provides in its appendix a list of OCs classified as asterisms, valuable information that is lost if only the candidate’s parameters are displayed in the catalogue.

5 CONCLUSIONS

We introduced the Unified Cluster Catalogue or UCC, along with its accompanying tool for membership probability estimation, the `fastMP` code. This catalogue represents the most extensive compilation of open clusters to date and will be regularly updated as new databases become publicly available in the scientific literature. The UCC is accessible through its dedicated website at <https://ucc.ar>, where each OC is presented along with its fundamental parameters, sourced from the literature whenever available. Users can interactively explore the data online through Python notebooks hosted on the Google Colaboratory service. In its initial version the UCC includes nearly 14000 unique candidate OCs, encompassing

⁹ Aladin: <http://aladin.cds.unistra.fr/>

¹⁰ SAO/NASA ADS: <https://ui.adsabs.harvard.edu/>

¹¹ CDS: <http://cdsportal.u-strasbg.fr/>

¹² Colaboratory: <https://colab.research.google.com/>

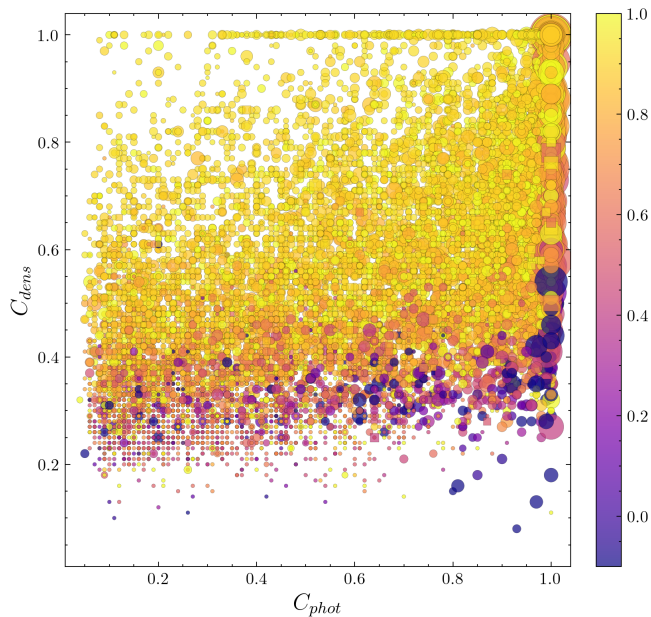


Figure 7. Five dimensional density C_{dens} versus photometry based metric C_{phot} for the candidate OCs listed in the UCC. Colour is related to the vertical distance to the total proper motion quality cut. The colourbar is clipped at -0.1 and 1 to improve visibility. Size is related to the spatial extension of its members. Squares are associated to candidates beyond the 20 pc spatial dispersion quality cut.

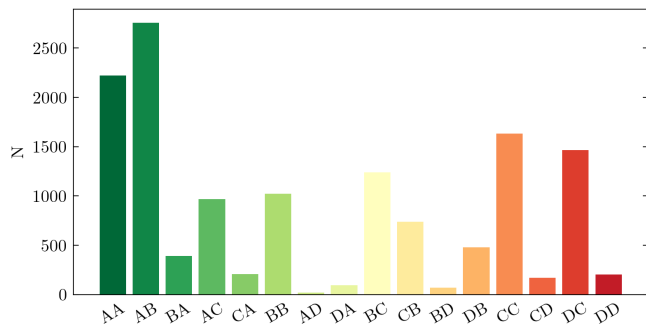


Figure 8. Distribution of the quality classes obtained combining the C_{phot} and C_{dens} values for each candidate OC as described in the text.

a combined total of over 1 million proposed member stars, averaging approximately ~ 90 member stars per OC.

Replacing the trained eye of a researcher even for the initial assessment of what constitutes a true OC in a completely generalized approach, is a formidable challenge. With hundreds or even thousands of new candidate OCs emerging in the literature every few months, the need for a systematic method to address this issue becomes increasingly crucial. Our classification parameters, C_{phot} and C_{dens} , were developed to assist in this task, but a thorough visual inspection remains essential, particularly for more complex objects. We anticipate that the Unified Cluster Catalogue and its associated online service will prove to be a valuable resource for the astrophysical research community. We welcome all suggestions for expanding and improving it in the future.

ACKNOWLEDGEMENTS

We thank the financial support from the University of La Plata (I+D 11/G148), as well as the financial support from the University of Rosario (PPCT 80020210300042UR). We also thank the financial support from the IALP (CONICET-UNLP). The authors would like to thank Dr Emily Hunt for her assistance with the processing of the HUNT23 database. This work has made use of data from the European Space Agency (ESA) mission *Gaia* (<https://www.cosmos.esa.int/gaia>), processed by the *Gaia* Data Processing and Analysis Consortium (DPAC, <https://www.cosmos.esa.int/web/gaia/dpac/consortium>). Funding for the DPAC has been provided by national institutions, in particular the institutions participating in the *Gaia* Multilateral Agreement. This research has made use of the WEBDA database, operated at the Department of Theoretical Physics and Astrophysics of the Masaryk University. This research has made use of the VizieR catalog access tool, operated at CDS, Strasbourg, France (Ochsenbein et al. 2000). This research has made use of “Aladin sky atlas” developed at CDS, Strasbourg Observatory, France (Bonnarel et al. 2000; Boch & Fernique 2014; Baumann et al. 2022). This research has made use of NASA’s Astrophysics Data System. This research made use of the Python language (van Rossum 1995) and the following packages: NumPy¹³ (Van Der Walt et al. 2011), SciPy¹⁴ (Jones et al. 2001), matplotlib¹⁵ (Hunter et al. 2007), scikit-learn¹⁶ (Pedregosa et al. 2011), ASteCA¹⁷ (Perren et al. 2015). This work made use of Astropy¹⁸ a community-developed core Python package and an ecosystem of tools and resources for astronomy (Astropy Collaboration et al. 2013, 2018, 2022).

DATA AVAILABILITY

The data underlying this article are available in the repositories associated to the Unified Cluster Catalogue, accessible at <https://github.com/ucc23>. The code employed to process the data and generate the images in this article can be found in the repositories for the fastMP code at <https://github.com/Gabriel-p/fastMP>, and in the repository for the article itself at https://github.com/gabriel-p-artcls/23-08_UCC. Any missing data file and/or code file can be requested to the corresponding author and we will gladly make it available.

REFERENCES

- Anders F., Castro-Ginard A., Casado J., Jordi C., Balaguer-Núñez L., 2022, *Research Notes of the AAS*, 6, 58
 Astropy Collaboration et al., 2013, *A&A*, 558, A33
 Astropy Collaboration et al., 2018, *AJ*, 156, 123
 Astropy Collaboration et al., 2022, *apj*, 935, 167
 Babusiaux C., et al., 2022, *arXiv e-prints*, p. arXiv:2206.05989
 Barbá R. H., et al., 2015, *A&A*, 581, A120
 Bastian U., 2019, *A&A*, 630, L8

¹³ <http://www.numpy.org/>

¹⁴ <http://www.scipy.org/>

¹⁵ <http://matplotlib.org/>

¹⁶ <https://scikit-learn.org/>

¹⁷ <https://github.com/asteca>

¹⁸ <http://www.astropy.org>

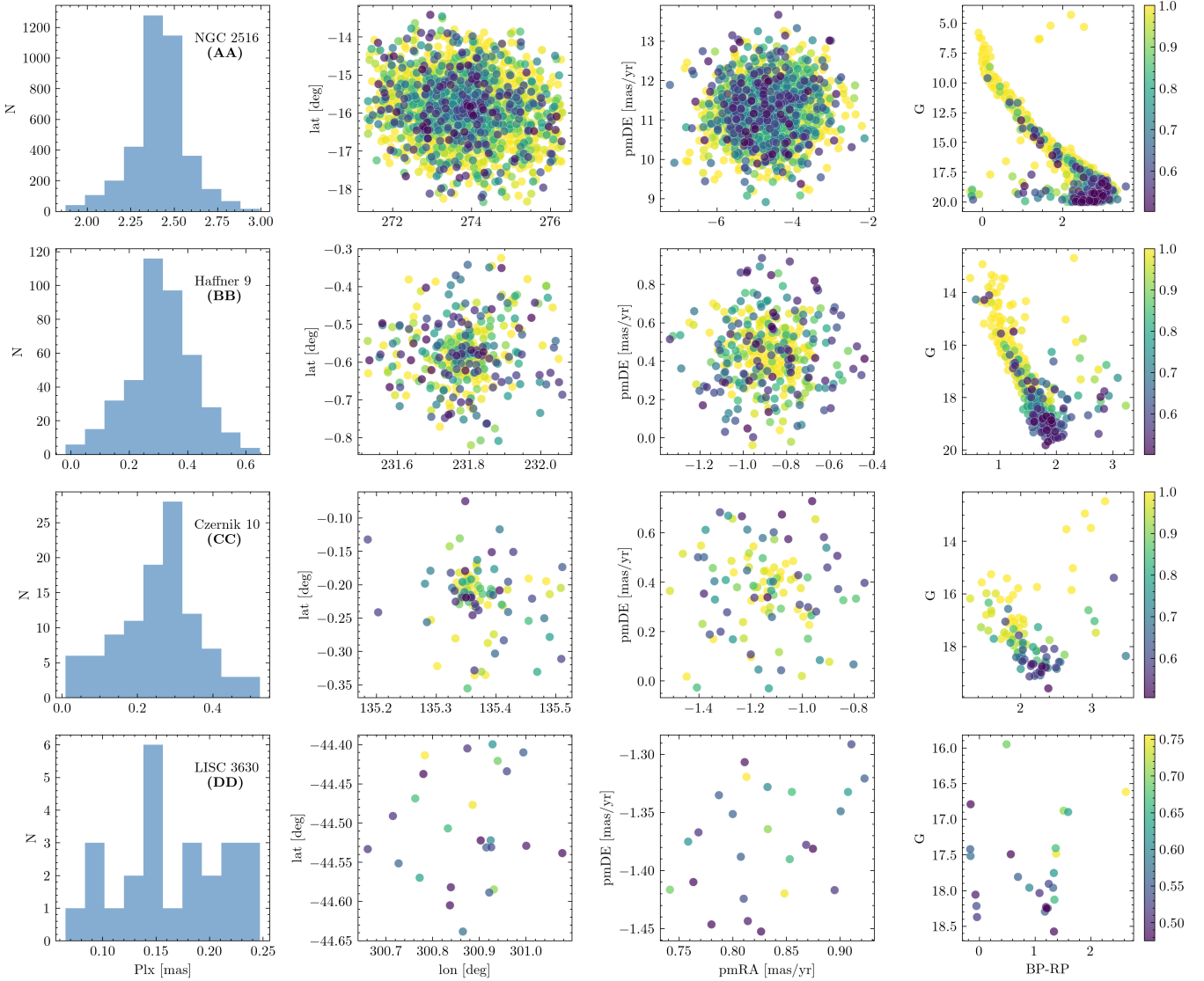


Figure 9. Examples of candidate OCs with combined classes AA, BB, CC, and DD from top to bottom rows, respectively. Plots show from left to right: parallax distribution, spatial dispersion, proper motions, and CMD. Colourbars are associated to the membership probabilities assigned by `fastMP`.

Baumann M., Boch T., Pineau F.-X., Fernique P., Bot C., Allen M., 2022, in Ruiz J. E., Pierfederici F., Teuben P., eds, *Astronomical Society of the Pacific Conference Series Vol. 532*, Astronomical Society of the Pacific Conference Series. p. 7

Bica E., Pavani D. B., Bonatto C. J., Lima E. F., 2019, *AJ*, **157**, 12

Boch T., Fernique P., 2014, in Manset N., Forshay P., eds, *Astronomical Society of the Pacific Conference Series Vol. 485*, *Astronomical Data Analysis Software and Systems XXIII*. p. 277

Bonatto C., Kerber L. O., Bica E., Santiago B. X., 2006, *A&A*, **446**, 121

Bonnarel F., et al., 2000, *AAPS*, **143**, 33

Campello R. J. G. B., Moulavi D., Sander J., 2013, in Pei J., Tseng V. S., Cao L., Motoda H., Xu G., eds, *Advances in Knowledge Discovery and Data Mining*. Springer Berlin Heidelberg, Berlin, Heidelberg, pp 160–172

Cantat-Gaudin T., Anders F., 2020, *A&A*, **633**, A99

Cantat-Gaudin T., et al., 2020, *A&A*, **640**, A1

Casado J., 2021, *Research in Astronomy and Astrophysics*, **21**, 117

Casado J., HENDY Y., 2023, *Monthly Notices of the Royal Astronomical Society*, **521**, 1399

Castro-Ginard A., Jordi C., Luri X., Julbe F., Morvan M., Balaguer-Núñez L., Cantat-Gaudin T., 2018, *A&A*, **618**, A59

Castro-Ginard A., Jordi C., Luri X., Cantat-Gaudin T., Balaguer-Núñez L., 2019, *A&A*, **627**, A35

Castro-Ginard A., et al., 2020, *A&A*, **635**, A45

Castro-Ginard A., et al., 2022, *A&A*, **661**, A118

Chi H., Wang F., Li Z., 2023a, *Research in Astronomy and Astrophysics*, **23**, 065008

Chi H., Wei S., Wang F., Li Z., 2023b, *ApJS*, **265**, 20

Chi H., Wang F., Wang W., Deng H., Li Z., 2023c, *ApJS*, **266**, 36

Dias W. S., Monteiro H., Moitinho A., Lépine J. R. D., Carraro G., Paurzen E., Alessi B., Vilella L., 2021, *MNRAS*, **504**, 356

Dreyer J. L. E., 1888, *Mem. RAS*, **49**, 1

Efron B., 1979, *The Annals of Statistics*, **7**, 1

Ester M., Kriegl H.-P., Sander J., Xu X., 1996, in *Knowledge Discovery and Data Mining*.

Ferreira F. A., Santos J. F. C., Corradi W. J. B., Maia F. F. S., Angelo M. S., 2019, *MNRAS*, **483**, 5508

Ferreira F. A., Corradi W. J. B., Maia F. F. S., Angelo M. S., Santos J. F. C. J., 2020, *MNRAS*, **496**, 2021

Ferreira F. A., Corradi W. J. B., Maia F. F. S., Angelo M. S., Santos J. F. C. J., 2021, *MNRAS*, **502**, L90

- Friel E. D., 1995, *ARA&A*, **33**, 381
- Froebrich D., Scholz A., Raftery C. L., 2007, *MNRAS*, **374**, 399
- Gaia Collaboration et al., 2016, *A&A*, **595**, A1
- Gaia Collaboration et al., 2022, *arXiv e-prints*, p. [arXiv:2208.00211](https://arxiv.org/abs/2208.00211)
- Gieles M., Portegies Zwart S. F., 2011, *MNRAS*, **410**, L6
- Gran F., et al., 2022, *MNRAS*, **509**, 4962
- Hao C., Xu Y., Wu Z., He Z., Bian S., 2020, *PASP*, **132**, 034502
- Hao C. J., et al., 2021, *A&A*, **652**, A102
- Hao C. J., Xu Y., Wu Z. Y., Lin Z. H., Liu D. J., Li Y. J., 2022, *A&A*, **660**, A4
- He Z.-H., Xu Y., Hao C.-J., Wu Z.-Y., Li J.-J., 2021, *Research in Astronomy and Astrophysics*, **21**, 093
- He Z., et al., 2022a, *ApJS*, **260**, 8
- He Z., Wang K., Luo Y., Li J., Liu X., Jiang Q., 2022b, *ApJS*, **262**, 7
- He Z., Luo Y., Wang K., Ren A., Peng L., Cui Q., Liu X., Jiang Q., 2023a, *arXiv e-prints*, p. [arXiv:2305.10269](https://arxiv.org/abs/2305.10269)
- He Z., Liu X., Luo Y., Wang K., Jiang Q., 2023b, *ApJS*, **264**, 8
- Herschel W., 1786, *Philosophical Transactions of the Royal Society of London Series I*, **76**, 457
- Høg E., et al., 1997, *A&A*, **323**, L57
- Huchra J. P., Geller M. J., 1982, *ApJ*, **257**, 423
- Hunt E. L., Reffert S., 2021, *A&A*, **646**, A104
- Hunt E. L., Reffert S., 2023, *A&A*, **673**, A114
- Hunter J. D., et al., 2007, *Computing in science and engineering*, **9**, 90
- Jaehrig K., Bird J., Holley-Bockelmann K., 2021, *ApJ*, **923**, 129
- Jones E., Oliphant T., Peterson P., et al., 2001, *SciPy: Open source scientific tools for Python*, <http://www.scipy.org/>
- Kharchenko N. V., Piskunov A. E., Schilbach E., Röser S., Scholz R. D., 2012, *A&A*, **543**, A156
- Kos J., et al., 2018, *MNRAS*, **480**, 5242
- Kounkel M., Covey K., Stassun K. G., 2020, *AJ*, **160**, 279
- Krone-Martins A., Moitinho A., 2014, *A&A*, **561**, A57
- Li Z., Mao C., 2023, *ApJS*, **265**, 3
- Li Z., et al., 2022, *ApJS*, **259**, 19
- Liu L., Pang X., 2019, *ApJS*, **245**, 32
- Lloyd S., 1982, *IEEE Transactions on Information Theory*, **28**, 129
- Loktin A. V., Popova M. E., 2017, *Astrophysical Bulletin*, **72**, 257
- Lynga G., 1987, *VizieR Online Data Catalog*, p. VII/92A
- MacQueen J., 1967, *Some methods for classification and analysis of multivariate observations*, Proc. 5th Berkeley Symp. Math. Stat. Probab., Univ. Calif. 1965/66, **1**, 281-297 (1967).
- Mermilliod J.-C., 1995, in Egret D., Albrecht M. A., eds, Vol. 203, *Information & On-Line Data in Astronomy*. p. 127, doi:10.1007/978-94-011-0397-8_12
- Messier C., 1774, *Mémoires de l'Académie Royale des Sciences*, pp 435–461
- Ochsenbein F., Bauer P., Marcout J., 2000, *A&AS*, **143**, 23
- Parker R. J., 2014, in *The Labyrinth of Star Formation*. p. 431 ([arXiv:1208.0011](https://arxiv.org/abs/1208.0011)), doi:10.1007/978-3-319-03041-8_86
- Pedregosa F., et al., 2011, *Journal of Machine Learning Research*, **12**, 2825
- Pera M. S., Perren G. I., Moitinho A., Navone H. D., Vazquez R. A., 2021, *A&A*, **650**, A109
- Perren G. I., Vázquez R. A., Piatti A. E., 2015, *A&A*, **576**, A6
- Perryman M. A. C., et al., 1997, *A&A*, **323**, L49
- Qin S.-M., Li J., Chen L., Zhong J., 2021, *Research in Astronomy and Astrophysics*, **21**, 045
- Qin S., Zhong J., Tang T., Chen L., 2023, *ApJS*, **265**, 12
- Ripley B. D., 1976, *Journal of Applied Probability*, **13**, 255–266
- Ripley B. D., 1979, *Journal of the Royal Statistical Society. Series B (Methodological)*, **41**, 368
- Ryu J., Lee M. G., 2018, *ApJ*, **856**, 152
- Santos-Silva T., et al., 2021, *MNRAS*, **508**, 1033
- Sim G., Lee S. H., Ann H. B., Kim S., 2019, *Journal of Korean Astronomical Society*, **52**, 145
- Skrutskie M. F., et al., 2006, *AJ*, **131**, 1163
- Tarricq Y., Soubiran C., Casamiuela L., Castro-Ginard A., Olivares J., Miret-Roig N., Galli P. A. B., 2022, *A&A*, **659**, A59
- Tian H.-J., 2020, *ApJ*, **904**, 196
- Tremmel M., et al., 2013, *ApJ*, **766**, 19
- Van Der Walt S., Colbert S. C., Varoquaux G., 2011, *Computing in Science & Engineering*, **13**, 22
- Vasiliev E., Baumgardt H., 2021, *MNRAS*, **505**, 5978
- Zari E., Hashemi H., Brown A. G. A., Jardine K., de Zeeuw P. T., 2018, *A&A*, **620**, A172
- van Rossum G., 1995, Report CS-R9526, Python tutorial. pub-CWI, pub-CWI:adr

APPENDIX A: DATABASES CLEANING

We describe here a summary of the cleaning and standardizing processes applied on almost all of the catalogues mentioned in Table 1. Most of these are small tasks, like manually editing names so that they are consistent across databases, but they were necessary (and rather time consuming). For convenience we abbreviate Kharchenko et al. (2012) as KHAR12 and Bica et al. (2019) as BICA19. The catalogue used for identifying globular clusters (GCs) is that of Vasiliev & Baumgardt (2021) with the addition of the Gran 2, 3, 4, and 5 objects from Gran et al. (2022).

Kharchenko et al. (2012): Selected all entries with *class* equal to “OPEN STAR CLUSTER”, resulting in 2858 entries. The astrometry values in this database are of low quality, we do not use these values in the membership estimation process. Added the preferred denomination VDBH to vdBergh-Hagen and VDB to vdBergh clusters, per CDS recommendation (this is done across all the catalogues). Removed entries that match Galactic clusters: ESO 456-29 (Gran 1), FSR 1716, FSR 1758, VDBH 140.

Loktin & Popova (2017): Many proper motion values in this catalogue are clearly wrong (e.g. the values for NGC 2516). We thus do not use these values in the membership estimation process. Removed entries that match Galactic clusters: Berkeley 42 (NGC 6749), Lynga 7 (BH 184). Fixed the name of four listed OCs: Sauer5 → Saurer 5, Teusch61 → Teutsch 61, AlessiJ2327+55 → Alessi J2327.0+55, Sigma Ori → Sigma Orionis.

Bica et al. (2019): The VizieR table contain 10978 entries, we keep only those with class OC (open cluster) or OCC (open cluster candidate). This reduces the list to 3564 entries.

This is the only DB that lists the Ryu & Lee (2018) clusters. The original article claims to have found 721 new OCs (923 minus 202 embedded). BICA19 (page 11) says that the Ryu & Lee article lists 719 OCs (921 minus 202 embedded). BICA19 lists in its VizieR table only 711 Ryu OCs, 4 of which are listed with alternative names (Teutsch J1814.6-2814 → Ryu 563, Quartet → Ryu 858, “GLIMPSE 70, Mercer 70” → Ryu 273, “LS 468|La Serena 468” → Ryu 094). Hence there are 707 Ryu clusters in the final BICA19 VizieR table. Removed entries: MWSC 2776, FSR 523, FSR 847, FSR 436 (listed twice, removed one of the entries); ESO 393-3 (listed twice and no available data in CDS to decide, removed both); MWSC 1025, 1482, 948, 3123, 1997, 1840, 442, 1808, 2204 (listed twice, removed name from both entries as they were not found in KHAR12); ESO 97-2 (removed from Loden 848 as it matches the position of Loden 894); FSR 972, OCL 344, Collinder 384, FSR 179 (listed twice, removed from both entries as we found no available data in CDS to check); MWSC 206 (listed twice, removed the entry that also showed FSR 60 since the coordinates for FSR 60 are a better match in KHAR12 for the entry with the single FSR 60 name); Alessi J0715.6-0722 (removed as its position matches that of Alessi J0715.6-0727).

Fixed the name of the following entries: FSR 429.MWSC 3667

→ FSR 429,MWSC 3667; Carraro 1.MWSC 1829 → Carraro 1,MWSC 1829; Cernik 39 → Czernik 39; de Wit 1 → Wit 1 (to match KHAR12); JS 1 → Juchert-Saloran 1 (to match KHAR12); ESO 589-26,MW → ESO 589-26; Alessi J2327.6+5535 → Alessi J2327.0+55; TRSG 1 → RSG 1; Dol-Dzim 9 added DoDz 9 (to match KHAR12); Dol-Dzim 11 added DoDz 11 (to match KHAR12). Removed entries that match GCs: ESO 456-29,MWSC 2761 (Gran 1); ESO 93-8,MWSC 1932; FSR 1758,MWSC 2617; VDBH 140,vdBergh-Hagen 140,FSR 1632,MWSC 2071.

[Sim et al. \(2019\)](#): Added a 'plx' column estimated as the inverse of the distance (the distance in parsecs is included in the catalogue).

[Liu & Pang \(2019, LIU19\)](#): Added the identifier 'FoF' to all the entries to match HUNT23. Changed 'LP' for 'FoF' in all the catalogues where it appeared, for consistency.

[Cantat-Gaudin et al. \(2020\)](#): Changed Sigma Ori → Sigma Orionis.

[Castro-Ginard et al. \(2020\)](#): Fixed wrong right ascension value for UBC 595 and UBC 181.

[Hao et al. \(2020\)](#): Added the acronym 'HXWHB' to match HUNT23.

[He et al. \(2021\)](#): Added 'CWNU' acronym for consistency across catalogues.

[Dias et al. \(2021\)](#): Lists 177 LIU19 clusters because it includes clusters not listed as new by the authors. We remove all except those listed as new in LIU19. Cluster LP 866 was duplicated (listed also as LP 0866), entry was removed. Changed Sigma Ori → Sigma Orionis.

[Hao et al. \(2021\)](#): This database contains dozens of duplicated entries and even some that are listed thrice, e.g: ESO 130-06, ESO 368-11, ESO 368-14 and Basel 11a. Furthermore, duplicated clusters are assigned very different fundamental parameters (e.g., Alessi 44 is listed twice and assigned logarithmic ages of 7.82 and 8.42). Of the almost 4000 listed OCs, ~15% show a difference in the mean parallax value with those from CANTAT20 larger than 50%. Finally some clusters have wildly incorrect astrometric parameters. For example the cluster Melotte 25 is assigned a parallax of 0.264 mas in this catalogue when its true value is larger than 21 mas. We thus unfortunately decided to exclude this catalogue from our list.

[Hao et al. \(2022\)](#): Removed the listed entry OC 0586 as a duplicate of the GC BH 140.

[Hunt & Reffert \(2023\)](#): Removed GCs listed as OCs: Palomar 2, 7 (listed as IC 1276) 8, 10, 11, 12; ESO 452-11 (1636-283); Pismis 26 (Ton 2); Lynga 7 (BH 184). New candidates HSC 2890 and HSC 134 were removed as their position and astrometry match those of the GCs Gran 3 and 4. Candidate HSC 2605 has very similar coordinates and proper motions to GC NGC 5139 but its parallax is different, so it was not removed. Removed moving groups and Theia objects from [Kounkel et al. \(2020\)](#). Fixed: ESO 429-429 → ESO 429-02 (position corresponds to this OC), AH03 J0748+26.9 → AH03 J0748-26.9, Juchert J0644.8+0925 → Juchert J0644.8-0925, Teutsch J0718.0+1642 → Teutsch J0718.0-1642, Teutsch J0924.3+5313 → Teutsch J0924.3-5313, Teutsch J1037.3+6034 → Teutsch J1037.3-6034, Teutsch J1209.3+6120 → Teutsch J1209.3-6120, Collinder 302 changed position to (RA=246.525, DEC=-26.233), it was centred on GC NGC 6121.

For ~160 HSC candidates we updated their centre values in coordinates. These are extended and irregular objects for which the median positions of their members was more than 1 deg away from the stored values in the HUNT23 database.

[Li & Mao \(2023\)](#): Database lists 56 'LISC' clusters but only 35 are kept as real objects. The parallax distances are in very bad agreement with the the estimated distance moduli. HUNT23 recovers 0% of these clusters. We keep the catalogue but advise caution.

[Chi et al. \(2023a\)](#): The article mentions 83 clusters but only 82 are visible in the article table that lists them. No Vizier data was available at the moment of writing this article and no answer was received after enquiring the author. answer. Added 'LISC-III' to the names to match HUNT23.

This paper has been typeset from a $\text{\TeX}/\text{\LaTeX}$ file prepared by the author.